

Analysis of controlled Rabi flopping in a double rephasing photon echo scheme for quantum memories

Rahmatullah^{1,2} and B. S. Ham^{1†}

¹Center for Photon Information Processing, and School of Electrical Engineering and Computer Science, Gwangju Institute of Science and Technology, Gwangju, Republic of Korea

²Department of Physics, COMSATS Institute of Information Technology, Islamabad, Pakistan

†E-mail: bham@gist.ac.kr

Keywords: Quantum optics, Coherent transients, Quantum memory, Photon echoes

Abstract

A double rephasing photon echo is analyzed for inversion-free photon echo-based quantum memories using controlled Rabi flopping, where the Rabi flopping is used for phase control of atom coherence. Unlike the rephasing-caused π -phase shift in a single rephasing scheme, the control Rabi flopping between the excited state and an auxiliary third state induces coherence inversion. Thus, the absorptive photon echo in a double rephasing scheme can be manipulated to be emissive via the controlled Rabi flopping. Here we present a quantum coherence control of atom phases in a double rephasing photon echo scheme for emissive photon echoes for quantum memory applications.

1. Introduction

Modified photon echoes have been intensively studied for quantum memory applications over the last decade since the first protocol of controlled reversible inhomogeneous broadening, where photon echo can be achieved by a counter-propagating control pulse set in a three-level Doppler [1] and non-Doppler [2] medium. Due to the inherent population inversion in photon echoes [3], resulting in quantum noises and violation of no cloning theorem [4], conventional photon echo itself cannot be directly applied to quantum memories. Compared with single atom-based quantum memory protocols, e.g., utilizing nuclear spins recently demonstrated in Si-based semiconductors [5], the photon echoes in rare-earth doped solids have benefits of multimode, ultrafast, and ultrahigh absorption [6]. To overcome the inherent population inversion in photon echoes, atomic frequency comb (AFC) echoes [7,8], gradient echoes [9,10], and controlled double rephasing (CDR) echoes [11,12] are presented for quantum memory applications. Because ultralong quantum memory is an essential component for long-distance quantum communications using quantum repeaters [13,14], a storage time extension has also been a critical issue [15-18]. As experimentally demonstrated by using dynamic decoupling (DD) [14] and optical locking via controlled coherence conversion (CCC) [19], the optical storage time can be extended up to spin population decay time.

The CCC theory has been proposed to convert an absorptive echo into an emissive one in a double rephasing (DR) photon echo scheme [11]. The DR photon echo scheme inherently gives the benefit of no population inversion. Because rephasing itself in photon echoes results in a time reversal process owing to a π phase shift in collective atom coherence, the DR echo is obviously absorptive like the data pulse due to the 2π phase shift (no change) in coherence. Although silent echoes in doubly rephased echo schemes have been successfully demonstrated [20-22], the final echo extraction out of the medium is strongly prohibited due to its absorptive coherence [11,12]. Moreover, there is no way to solve this absorptive echo problem in a two-level system, at least not yet. However, DR photon echoes have been observed recently, which is seemingly violating the CDR echo theory. In the photon echo experiments, however, echoes are always observed

regardless of the pulse area due to the imperfect rephasing-caused coherence leakage when commercial Gaussian lights are used. Recently calculated Gaussian pulse-caused echo efficiency is as high as 26% in the double rephasing scheme [23]. The CCC in CDR echoes has already been discussed in a single rephasing photon echo scheme theoretically [24] as well as experimentally [25].

Here in the present paper, we analytically investigate the collective atom phase control in a DR scheme, and confirm the CDR echo theory with a proof of coherence inversion. Compared with full numerical analysis in previous discussions [11,12,16,17,24], we present full analytic solutions in this article.

2. Theory

Figure 1 is a schematic diagram of the present CDR echoes, where the control pulse set of C_1 and C_2 is for the atom phase control in the DR scheme. The data (D), first rephasing (R_1) and second rephasing (R_2) pulses satisfy a double rephasing photon echo scheme, where they are resonant between states $|1\rangle$ and $|2\rangle$ as shown in Fig. 1(a). The pulse sequence of CDR is shown in Fig. 1(b), where the control pulse set C_1 and C_2 is resonant between states $|2\rangle$ and $|3\rangle$. The time delay τ between C_1 and C_2 is used for storage time extension, which is limited by the spin dephasing [25,26]. The spin dephasing can be minimized with the zero first-order Zeeman method [27]. In an optical locking scheme applied to three-pulse photon echoes [17], the storage time extends up to spin population decay time [19]. To satisfy general conditions of CDR, each pulse area of R_1 , R_2 , C_1 , and C_2 is set to be π . The pulse area of D is set to small at 0.1π . The pulse area is defined by $\varphi_i = \int \Omega_i dt$, and Ω_i ($i = D, R_1, R_2, C_1$ and C_2) is the Rabi frequency of the pulse.

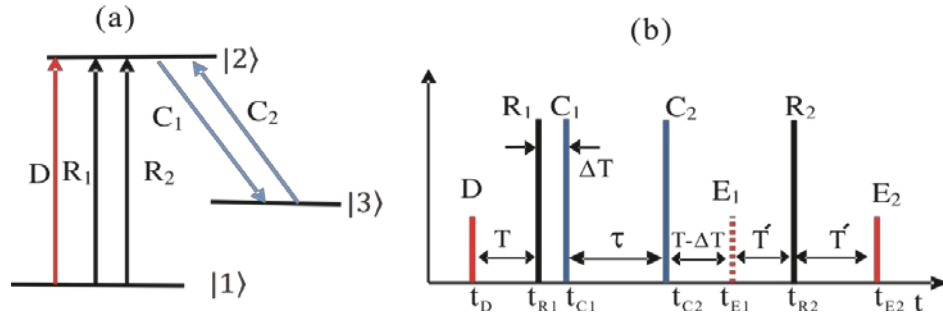


Figure 1. (a) Schematic of controlled double rephasing echoes. (b) Pulse sequence for (a). t_j is the the arrival time of pulse j .

The CCC in CDR must be distinguished from resonant Raman or electromagnetically induced transparency (EIT) based on two-photon resonance without shelving on the excited state. For photon echo-based quantum memories, the signal (data) pulse information (phase and amplitude) must be fully transferred into a matter (optical coherence) state via a complete absorption process in an optically dense, inhomogeneously broadened two-level medium [16]. Unlike other coherence optics in a three-level system mentioned above, the inhomogeneity of the ensemble is the fundamental requirement for the coherence evolutions in photon echoes. One unique property of the CCC is the double coherence swapping between the optical and spin states via the control pulse set of C_1 and C_2 . Unlike EIT, The R_1 and C_1 must be avoided from the two-photon Raman coherence, where the delay ΔT between R_1 and C_1 must be longer than the inverse of inhomogeneous width. Usually this requirement is easily satisfied even for the consecutive π -optical pulse sequence in most rare-earth doped solids [25].

The purpose of C_1 is simply to hold both optical phase decay and optical phase evolutions via complete population transfer from the excited state $|2\rangle$ to the auxiliary spin state $|3\rangle$, resulting

in optical coherence $\rho_{12}=0$ [11]. For this the state $|3\rangle$ must be vacant initially. When the second control pulse C_2 is turned on, the system population is completely recovered to the initial one reached by R_1 . However, the system coherence is not invariant, resulting in absorptive photon echo E_2 [12,24].

The interaction picture Hamiltonian in the atom-field interactions under rotating-wave approximation of the proposed system in Fig. 1(a) is written as:

$$H = -\hbar/2 \begin{bmatrix} 0 & \Omega_j & 0 \\ \Omega_j & 0 & \Omega_k \\ 0 & \Omega_k & 0 \end{bmatrix}, \quad (1)$$

where, $\Omega_j(j= D, R_1 \text{ or } R_2)$ is the Rabi frequency of D, R_1 and R_2 , or $\Omega_k(k= C_1 \text{ or } C_2)$ is the Rabi frequency of C_1 or C_2 . We calculate the rate equations for the density matrix elements using Von Neumann equation [28]:

$$\dot{\rho} = -\frac{i}{\hbar}[H, \rho] - \frac{1}{2}\{\Gamma, \rho\}. \quad (2)$$

The corresponding rate equations are

$$\dot{\rho}_{11} = -i\frac{\Omega_j}{2}(\rho_{12} - \rho_{21}), \quad (3a)$$

$$\dot{\rho}_{22} = -i\frac{\Omega_j}{2}(\rho_{21} - \rho_{12}) - i\frac{\Omega_k}{2}(\rho_{23} - \rho_{32}), \quad (3b)$$

$$\dot{\rho}_{33} = -i\frac{\Omega_k}{2}(\rho_{32} - \rho_{23}), \quad (3c)$$

$$\dot{\rho}_{12} = -i\frac{\Omega_j}{2}(\rho_{11} - \rho_{22}) - i\frac{\Omega_k}{2}\rho_{13}, \quad (3d)$$

$$\dot{\rho}_{12} = -i\frac{\Omega_k}{2}\rho_{12} + i\frac{\Omega_j}{2}\rho_{23}, \quad (3e)$$

$$\dot{\rho}_{23} = -i\frac{\Omega_k}{2}(\rho_{22} - \rho_{33}) + i\frac{\Omega_j}{2}\rho_{13}, \quad (3f)$$

where, all decay rates are set to be zero for simplicity. Thus the the overall dephasing is only due to the atom detuning in the inhomogeneous broadening. We now consider the CDR echo scheme for the following discussion. For this we start with a general DR scheme to investigate the absorptive coherence on the final echo E_2 without C_1 and C_2 pulses in Fig. 1.

3. Discussion

3.1. DR photon echoes

In this sub-section, we study conventional two-pulse photon echoes in a DR scheme without C_1 and C_2 in Fig. 1. We derive time-dependent density matrix equations for the expressions of ensemble coherence between the ground and excited states, and population in each bare state.

3.1.1. D-pulse

We first derive the expressions of coherence and population excited by the D-pulse. The equations of motion for D-pulse by setting $\Omega_j = \Omega_D$ and $\Omega_k = 0$ in equation (3) are as follows:

$$\dot{\rho}_{11} = -i\frac{\Omega_D}{2}(\rho_{12} - \rho_{21}), \quad (4a)$$

$$\dot{\rho}_{22} = -i \frac{\Omega_D}{2} (\rho_{21} - \rho_{12}), \quad (4b)$$

$$\dot{\rho}_{12} = -i \frac{\Omega_D}{2} (\rho_{11} - \rho_{22}), \quad (4c)$$

$$\dot{\rho}_{21} = -i \frac{\Omega_D}{2} (\rho_{22} - \rho_{11}). \quad (4d)$$

Initially all atoms are in the ground state $|1\rangle$: $\rho_{11}(0) = 1$; $\rho_{22}(0) = \rho_{12}(0) = \rho_{21}(0) = 0$. The Laplace transform of equation (4) with $\rho_{11} + \rho_{22} = 1$ yields:

$$\mathcal{L}[\rho_{11}] = \frac{2s^2 + \Omega_D^2}{2s(s^2 + \Omega_D^2)}, \quad (5a)$$

$$\mathcal{L}[\rho_{12}] = \frac{-i\Omega_D}{(s^2 + \Omega_D^2)}, \quad (5b)$$

$$\mathcal{L}[\rho_{21}] = \frac{i\Omega_D}{(s^2 + \Omega_D^2)}. \quad (5c)$$

The final equations for population and coherence are obtained by taking the inverse Laplace transform of equation (5):

$$\rho_{11} = \cos^2\left(\frac{\varphi_D}{2}\right), \quad (6a)$$

$$\rho_{22} = \sin^2\left(\frac{\varphi_D}{2}\right), \quad (6b)$$

$$\rho_{12} = -\frac{i}{2} \sin(\varphi_D), \quad (6c)$$

where φ_D is the area of the D-pulse. The D-pulse obeys the area theorem which has a direct relation with coherence [29]:

$$\frac{\partial \varphi_D}{\partial z} = -\frac{\alpha}{2} \sin(\varphi_D), \quad (7)$$

where α is the absorption coefficient. For the D-pulse with a very small pulse area, $\sin(\varphi_D) \approx 1$, $\varphi_D = (\varphi_D)_0 e^{-\alpha z/2}$ represents the Beer's law. The information of D-pulse is now transferred into the atom coherence. For a weak D-pulse, $\varphi_D \ll 1$, the atomic population still remains in the ground state $|1\rangle$: $\rho_{11} \approx 1$; $\rho_{22} \approx 0$. In our analysis, the D-pulse area is set to be 0.1π .

3.1.2. R₁-pulse

As soon as the atoms are excited by D, they immediately start to evolve with their own detuning-dependent phase velocity until the rephasing pulse (R₁-pulse) comes. We use equation (6) as initial conditions for $\Omega_j = \Omega_{R_1}$ and $\Omega_k = 0$ to solve equation (3). The solution of the rate equations for R₁-pulse is as followings:

$$\rho_{11} = \cos^2\left(\frac{\varphi_D + \varphi_{R_1}}{2}\right), \quad (8a)$$

$$\rho_{22} = \sin^2\left(\frac{\varphi_D + \varphi_{R_1}}{2}\right), \quad (8b)$$

$$\rho_{12} = -\frac{i}{2} \sin(\varphi_D + \varphi_{R_1}). \quad (8c)$$

Equation (8c) indicates that the rephasing π pulse R_1 results in a π phase shift in the coherence ρ_{12} initiated by the D-pulse in equation (6c), as shown in Fig. 2(a): $[\rho_{12}] \xrightarrow{R_1} [\rho_{12}]^*$ (see also Appendix A for $\pi/2$ pulse area of D). All details of detuning-dependent atom phase evolutions and rephasing effects are numerically shown in Fig. 4 of ref. [24], where the real part of ρ_{12} is exactly symmetric, cancelling coherence each other. The π rephasing pulse swaps the population between ground and excited states as shown in Fig. 2(b), resulting in spontaneous and/or stimulated emission noises. To overcome the population inversion, a controlled double rephasing concept has been developed in the name of CDR echoes [11,12]. For DR echoes, the second π optical pulse R_2 is added to swap the populations again, where the second echo E_2 is free from quantum noises. To fully restore the D-pulse transferred coherence, the first echo E_1 must be erased (or silenced), where this erasing process does not affect the individual coherence evolutions [20-22].

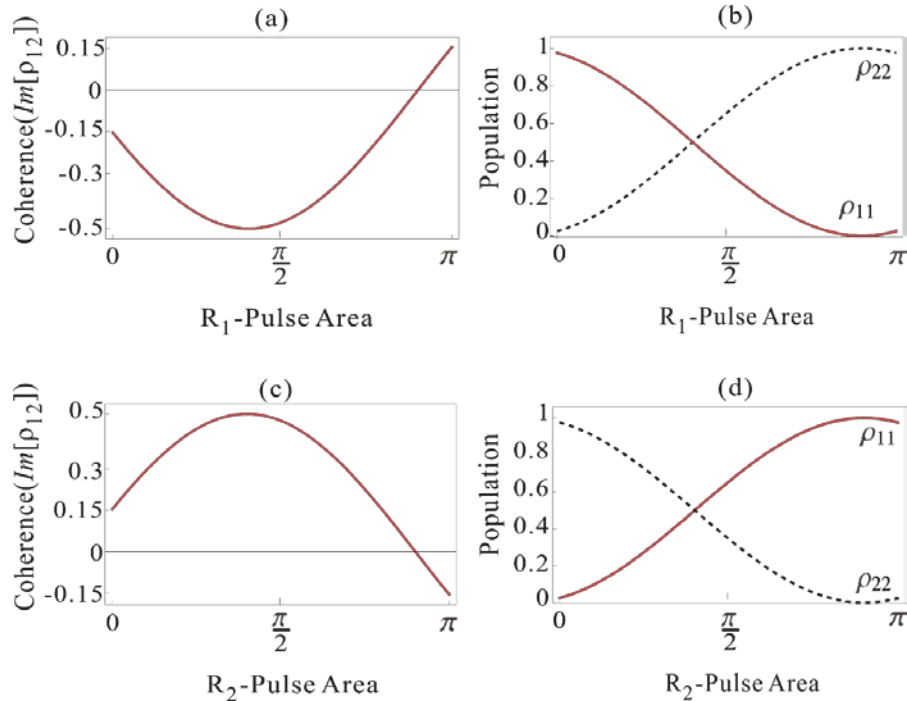


Figure 2. (a) Plot of $\text{Im}[\rho_{12}]$ (equation 8c) versus R_1 -pulse area φ_{R_1} with area of D-pulse $\varphi_D = 0.1\pi$. (b) Corresponding population evolution (red) ρ_{11} (equation 8a) and (dotted) ρ_{22} (equation 8b). (c) Plot of $\text{Im}[\rho_{12}]$ (equation 9c) versus R_2 -pulse area φ_{R_2} with area of D-pulse $\varphi_D = 0.1\pi$ and R_1 is $\varphi_{R_1} = \pi$. (d) Corresponding population evolution (red) ρ_{11} (equation 9a) and dotted ρ_{22} (equation 9b).

We derive the coherence and population rate equations for R_2 -pulse by replacing Ω_j with Ω_{R_2} and setting $\Omega_k = 0$ in equation (3). We use equation (8) as initial conditions and calculate the expressions for coherence and populations as follows:

$$\rho_{11} = \cos^2\left(\frac{\varphi_D + \varphi_{R_1} + \varphi_{R_2}}{2}\right), \quad (9a)$$

$$\rho_{22} = \sin^2\left(\frac{\varphi_D + \varphi_{R_1} + \varphi_{R_2}}{2}\right), \quad (9b)$$

$$\rho_{12} = -\frac{i}{2}\sin(\varphi_D + \varphi_{R_1} + \varphi_{R_2}). \quad (9c)$$

In Figs. 2(c) and (d), the R_2 pulse area-dependent coherence and population are shown for $\varphi_D = 0.1\pi$ and $\varphi_{R_1} = \pi$. As shown in Fig. 2(c), the π - R_2 pulse inverts the coherence as π - R_1 pulse does. Here, the negative sign in the coherence ρ_{12} shows absorption. Thus the second echo by R_2 is absorptive like the data pulse D [11,12]. This means that the generated echo E_2 in the DR scheme cannot be radiated out of the medium, as D is fully absorbed into the medium. By the way, the observations of E_2 in refs. [20-22] have been understood as imperfect rephasing-caused coherence leakage due to Gaussian distributed light pulses [23]. Our aim is here, to get the inversion-free emissive echo. To convert the absorptive echo E_2 in Fig. 2 into an emissive one, the CDR echo scheme is applied. In the following section, we describe the role of C_1 and C_2 for CCC in details.

3.2 CDR echoes

In this sub-section, we discuss the CDR echo of Fig. 1 by inserting the control pulse set of C_1 and C_2 in the DR scheme. The control pulse set can follow either R_1 as shown in Fig. 1(b) or R_2 as discussed in refs. [11,12]. In both cases, C_1 must be activated before the echo timing [24].

3.2.1. C_1 -pulse

The function of C_1 -pulse with a π pulse area is to temporally hold optical coherence decay as well as optical phase evolution via transferring population in the excited state $|2\rangle$ to an auxiliary ground (spin) state $|3\rangle$. In general, spin phase decay time is much longer than the optical counterpart in rare-earth doped crystals. Thus, C_1 plays a role of storage time extension [2,25,26]. The coherence and population changes by C_1 can be obtained by using equation (8) as initial conditions. The solutions of density matrix equation (3) for C_1 are obtained as:

$$\rho_{11} = \cos^2\left(\frac{\varphi_D + \varphi_{R_1}}{2}\right), \quad (10a)$$

$$\rho_{22} = \cos^2\left(\frac{\varphi_{C_1}}{2}\right)\sin^2\left(\frac{\varphi_D + \varphi_{R_1}}{2}\right), \quad (10b)$$

$$\rho_{33} = \sin^2\left(\frac{\varphi_{C_1}}{2}\right)\sin^2\left(\frac{\varphi_D + \varphi_{R_1}}{2}\right), \quad (10c)$$

$$\rho_{12} = -\frac{i}{2}\cos\left(\frac{\varphi_{C_1}}{2}\right)\sin(\varphi_D + \varphi_{R_1}), \quad (10d)$$

$$\rho_{13} = -\frac{1}{2}\sin\left(\frac{\varphi_{C_1}}{2}\right)\sin(\varphi_D + \varphi_{R_1}), \quad (10e)$$

$$\rho_{23} = -\frac{i}{2}\sin(\varphi_{C_1})\sin^2\left(\frac{\varphi_D + \varphi_{R_1}}{2}\right). \quad (10f)$$

The optical coherence ρ_{12} in equation (10d) by C_1 -pulse is equal to $\cos(\varphi_{C_1}/2)$ times the coherence generated by R_1 -pulse in equation (8c), where the R_1 -resulted coherence is 0.15 for the 0.1π of D-pulse and π of R_1 -pulse (see Fig. 3). So equation (10d) becomes $\rho_{12} = 0.15i \cos(\varphi_{C_1}/2)$ (see also Fig. 2(a)). Similarly the spin coherence in equation (10-e) is $\rho_{13} = 0.15 \sin(\varphi_{C_1}/2)$. In the absence of the C_1 -pulse, i.e., $\varphi_{C_1} = 0$, $\rho_{12} = 0.15i$ and $\rho_{13} = 0$. In the presence of the π C_1 -pulse, the optical and spin coherence becomes $\rho_{12} = 0.15i \cos(\pi/2) = 0$ and $\rho_{13} = 0.15 \sin(\pi/2) = 0.15ie^{-i\pi/2}$, respectively. Thus, the π - C_1 pulse adds a $\pi/2$ phase shift to the transferred coherence ρ_{13} [28]. This is a well-known property in a resonant two filed interactions in a three-

level atomic system, where there is a $\pi/2$ phase shift between Imp_{12} and Rep_{13} . In conclusion, C_1 pulse locks both optical phase decay and coherence evolutions, while transfers ρ_{12} into ρ_{13} with a $\pi/2$ phase shift via complete population transfer. In other words Imp_{12} becomes Rep_{13} as shown in Fig. 3(a). Here Imp_{13} is zero as Rep_{12} is zero in equation (6).

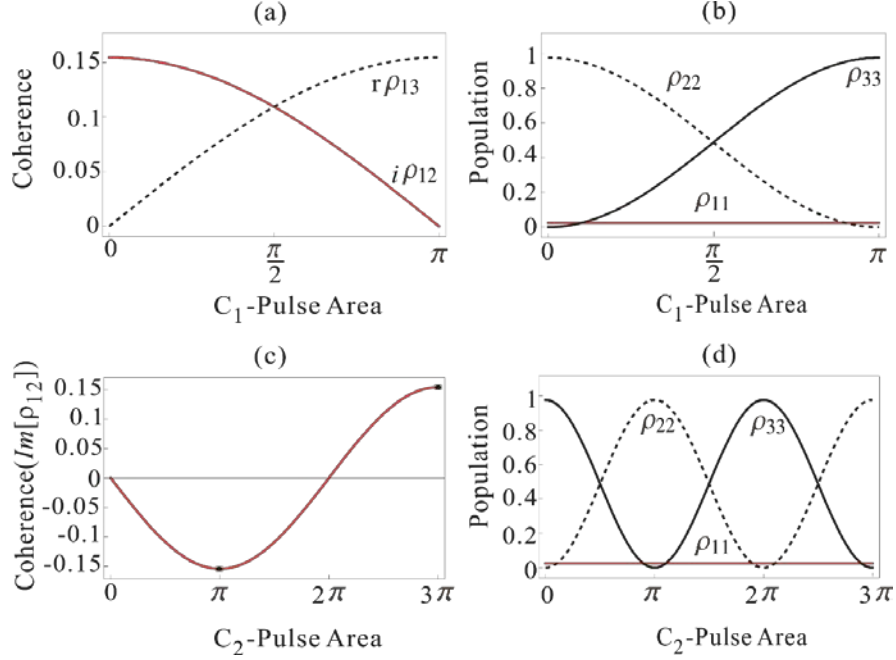


Figure 3. (a) Plot of $Im[\rho_{12}]$ and $Re[\rho_{13}]$ (equation 10d and 10e) versus C_1 -pulse area φ_{C_1} with area of D-pulse $\varphi_D = 0.1\pi$ and R_1 is $\varphi_{R_1} = \pi$. (b) Corresponding population evolution (red) ρ_{11} (equation 10a), (dotted) ρ_{22} (equation 10b) and (black) ρ_{33} (equation 10c). (c) Plot of $Im[\rho_{12}]$ (equation 11d) versus C_2 -pulse area φ_{C_2} with area of the other pulses are $\varphi_D = 0.1$, $\varphi_{R_1} = \pi$ and $\varphi_{C_1} = \pi$. (d) Corresponding population evolution (red) ρ_{11} (equation 11a), (dotted) ρ_{22} (equation 11b) and (black) ρ_{33} (equation 11c).

3.2.2. C_2 -pulse

The function of C_2 -pulse is to restore the transferred coherence by C_1 . Using equation (10) as initial conditions, and by setting $\Omega_k = \Omega_{C_2}$ and $\Omega_j = 0$ in equation (3), the system coherence and population expressions by C_2 -pulse are obtained as follows:

$$\rho_{11} = \cos^2\left(\frac{\varphi_D + \varphi_{R_1}}{2}\right), \quad (11a)$$

$$\rho_{22} = \cos^2\left(\frac{\varphi_{C_1} + \varphi_{C_2}}{2}\right) \sin^2\left(\frac{\varphi_D + \varphi_{R_1}}{2}\right), \quad (11b)$$

$$\rho_{33} = \sin^2\left(\frac{\varphi_{C_1} + \varphi_{C_2}}{2}\right) \sin^2\left(\frac{\varphi_D + \varphi_{R_1}}{2}\right), \quad (11c)$$

$$\rho_{12} = -\frac{i}{2} \cos\left(\frac{\varphi_{C_1} + \varphi_{C_2}}{2}\right) \sin(\varphi_D + \varphi_{R_1}), \quad (11d)$$

$$\rho_{13} = -\frac{1}{2} \sin\left(\frac{\varphi_{C_1} + \varphi_{C_2}}{2}\right) \sin(\varphi_D + \varphi_{R_1}), \quad (11e)$$

$$\rho_{23} = -\frac{i}{2} \sin(\varphi_{C_1} + \varphi_{C_2}) \sin^2\left(\frac{\varphi_D + \varphi_{R_1}}{2}\right). \quad (11f)$$

The coherence in equation (11d) is equal to $\cos((\varphi_{C_1} + \varphi_{C_2})/2)$ multiply by the coherence excited by R_1 -pulse in equation (8c). The π - π pulse sequence of C_1 and C_2 , therefore, induces a coherence inversion via the round trip of population transfer between the excited and auxiliary states: $\cos((\pi + \pi)/2) = -1$ (see Fig. 3(c) [11,12,24]: $\rho_{12} \xrightarrow{C_1 \& C_2} -\rho_{12}$). This coherence inversion mechanism is completely different from the rephasing by R_1 or R_2 [12]. In order to resume the coherence initiated by the R_1 -pulse, the sum pulse area of C_1 and C_2 must be equal to $4n\pi$ ($n = 1, 2, 3 \dots$). In Figs. 3(c) and 3(d), we plot the coherence and population as a function of the C_2 -pulse area for $\varphi_D = 0.1\pi$, $\varphi_{R_1} = \pi$ and $\varphi_{C_1} = \pi$. Figure 3(c) shows that the ensemble coherence excited by D and rephased by R_1 is recovered with 3π C_2 -pulse. The 3π C_2 , of course, returns the population from state $|3\rangle$ to the excited state $|2\rangle$ as shown in Fig. 3(d). Thus, the $(\pi$ - $\pi)$ C_1 - C_2 pulse sequence in controlled AFC [26] induces an absorptive echo as in the DR scheme in Fig. 2(c) due to the π phase shift by the control Rabi flopping. The experimental observation in ref. [26] is not an artifact but due to the coherence leakage by imperfect rephasing by commercial Gaussian distributed laser pulses, where its maximum echo efficiency is far less than unity [23]. In the CDR echo scheme, however π - π pulse sequence of C_1 and C_2 is required to compensate the π phase shift in the DR scheme.

3.2.3. R_2 -pulse

For the CDR echo in Fig. 1, the final analytic solutions of density matrix equation (3) are obtained by using equation (11) as initial conditions:

$$\begin{aligned} \rho_{11} = & \frac{1}{16} \left[\cos\left(\frac{\varphi_{C_1} + \varphi_{C_2} - \varphi_D - \varphi_{R_2} - \varphi_{R_1}}{2}\right) - \cos\left(\frac{\varphi_{C_1} + \varphi_{C_2} - \varphi_D + \varphi_{R_2} - \varphi_{R_1}}{2}\right) + \right. \\ & 2 \cos\left(\frac{\varphi_D - \varphi_{R_2} + \varphi_{R_1}}{2}\right) - \cos\left(\frac{\varphi_{C_1} + \varphi_{C_2} + \varphi_D - \varphi_{R_2} + \varphi_{R_1}}{2}\right) + \\ & \left. \cos\left(\frac{\varphi_{C_1} + \varphi_{C_2} + \varphi_D + \varphi_{R_2} - \varphi_{R_1}}{2}\right) + 2 \cos\left(\frac{\varphi_D + \varphi_{R_2} + \varphi_{R_1}}{2}\right) \right]^2, \end{aligned} \quad (12a)$$

$$\begin{aligned} \rho_{22} = & \frac{1}{16} \left[\sin\left(\frac{\varphi_{C_1} + \varphi_{C_2} - \varphi_D - \varphi_{R_2} - \varphi_{R_1}}{2}\right) + \sin\left(\frac{\varphi_{C_1} + \varphi_{C_2} - \varphi_D + \varphi_{R_2} - \varphi_{R_1}}{2}\right) + \right. \\ & 2 \sin\left(\frac{\varphi_D - \varphi_{R_2} + \varphi_{R_1}}{2}\right) - \sin\left(\frac{\varphi_{C_1} + \varphi_{C_2} + \varphi_D - \varphi_{R_2} + \varphi_{R_1}}{2}\right) - \\ & \left. \sin\left(\frac{\varphi_{C_1} + \varphi_{C_2} + \varphi_D + \varphi_{R_2} + \varphi_{R_1}}{2}\right) - 2 \sin\left(\frac{\varphi_D + \varphi_{R_2} + \varphi_{R_1}}{2}\right) \right]^2, \end{aligned} \quad (12b)$$

$$\rho_{33} = \sin^2\left(\frac{\varphi_{C_1} + \varphi_{C_2}}{2}\right) \sin^2\left(\frac{\varphi_D + \varphi_{R_1}}{2}\right), \quad (12c)$$

$$\rho_{12} = -\frac{i}{16} \left[2 \sin(\varphi_{R_2}) + 2 \sin(\varphi_{R_2}) \cos(\varphi_D + \varphi_{R_1}) \left(3 + \cos\left(\frac{\varphi_{C_1} + \varphi_{C_2}}{2}\right) \right) + \sin(\varphi_{C_1} + \varphi_{C_2} - \varphi_{R_2}) - \sin(\varphi_{C_1} + \varphi_{C_2} + \varphi_{R_2}) + 8 \cos(\varphi_{R_2}) \sin(\varphi_D + \varphi_{R_1}) \cos\left(\frac{\varphi_{C_1} + \varphi_{C_2}}{2}\right) \right]. \quad (12d)$$

In Fig. 4, we plot the evolutions of coherence and population as a function of R_2 -pulse area for $\varphi_D = 0.1\pi$, $\varphi_{R_1} = \pi$, $\varphi_{C_1} = \pi$ and $\varphi_{C_2} = \pi$. As a result, both coherence and population excited by D are recovered with a π pulse area of R_2 , where spontaneous and stimulated emission-caused quantum noises are completely eliminated.

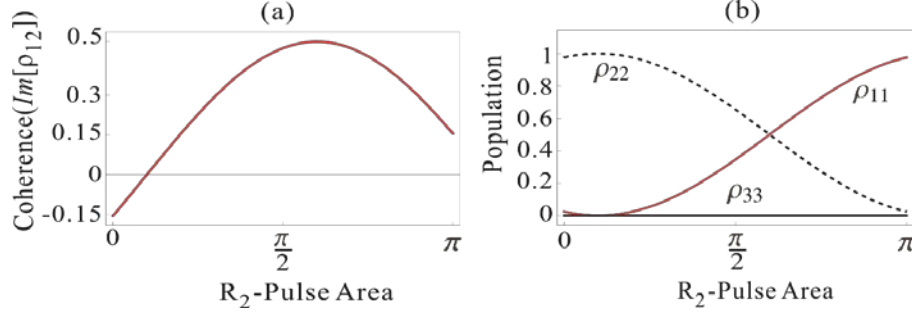


Figure 4. (a) Plot of $\text{Im}[\rho_{12}]$ (equation 12d) versus R_2 -pulse area φ_{R_2} . The area of other pulses are $\varphi_D = 0.1$, $\varphi_{R_1} = \pi$, $\varphi_{C_1} = \pi$ and $\varphi_{R_2} = \pi$. (b) Corresponding population evolution (red) ρ_{11} (equation 12a), (dotted) ρ_{22} (equation 12b) and (black) ρ_{33} (equation 12c).

The present scheme can experimentally be realized in a rare-earth Pr^{3+} -doped Y_2SiO_5 . In most rare-earth doped media, the ground state hyperfine splitting is a few tens of magahertz. Thus, tens of GHz of optical inhomogeneous broadening can be sliced into many spectral channels for multiple quantum memories, where practical parameter of optical Rabi frequency is $\sim\text{MHz}$. For an extended storage time by C_1 , Zeeman states may be used [29].

In an atomic ensemble such as Rb vapors, Zeeman splitting may also be used, where optical polarization control has been adapted to form a three-level system. However, such an atomic medium may not a good candidate for the photon echo-based quantum memory applications simply due to fast atomic diffusion. Moreover, providing a π optical pulse in a few ns pulse duration within the optical phase decay time is very challenging with a commercial cw laser system.

4 Conclusion

In conclusion, we analytically presented the CDR echo protocol for spontaneous emission-free-photon echo-based quantum memory applications by combining double rephasing photon echoes with control Rabi flopping. For this, time-dependent density matrix equations were analytically solved for coherence/population evolutions to investigate the phase shift of a resonant atom. To overcome the absorptive echo problem in a bare double rephasing photon echo scheme, consecutive π - π control pulse sequence is inserted right after the first rephasing pulse. The control pulse-generated π phase shift was exactly compensated with another π phase shift resulted from the double rephasing scheme. As a result emissive photon echoes were obtained under no population inversion.

Acknowledgment

This work was supported by the ICT R&D program of MSIP/IITP (1711028311: Reliable cryptosystem standards and core technology development for secure quantum key distribution network.

APPENDIX A: Coherence swapping using $\pi/2$ D-pulse

Here we analyze the coherence swapping by the π control pulse C_1 for a $\pi/2$ D-pulse in Fig. 3. The $\pi/2$ D-pulse creates maximum coherence between $|1\rangle \leftrightarrow |2\rangle$ transition, where $\text{Im}[\rho_{12}] = -0.5$ (see equation (6c) for $D = \pi/2$). The negative sign represents absorption of the D-pulse. In Fig. 5, we show a phase shift of the D-pulse excited coherence according to each applied pulses. The first rephasing pulse R_1 switches the coherence from absorption to emission as shown in Fig. 5(a).

Identical C_1 and C_2 pulses with π pulse area each invert the sign of coherence obtained by R_1 , resulting in an absorptive echo in Figs. 5(b) and (c). Finally, the second rephasing pulse R_2 adds a π phase shift to make the emissive photon echo under no population inversion as shown in Fig. 5(d). Either control pulse set or double rephasing pulse set with a 2π pulse area each does not change the D-excited population distribution. Thus, the CDR echo is confirmed for a noise free quantum memory protocol.

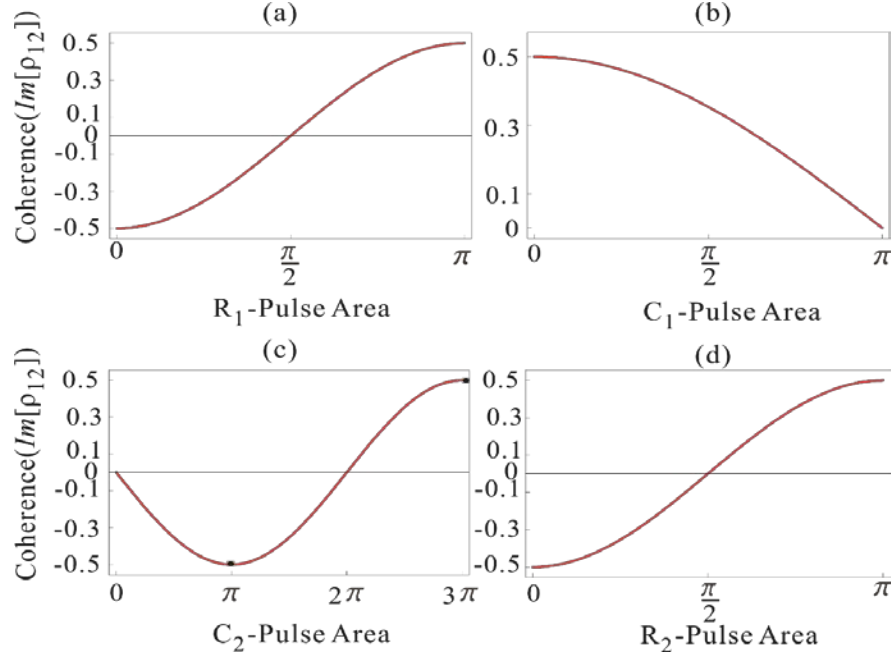


Figure 5. (a) Plot of $\text{Im}[\rho_{12}]$ versus (a) R_1 -pulse area φ_{R_1} (equation 8c), (b) C_1 -pulse area φ_{C_1} (equation 10d), (c) C_2 -pulse area φ_{C_2} (equation 11d) and R_2 -pulse area φ_{R_2} (equation 12d). The area of D-pulse is $\varphi_D = \pi/2$.

References

- [1] Moiseev S A and Kröll, S 2001 complete reconstruction of the quantum state of a single-photon wave packet absorbed by a Doppler-broadened transition. *Phys. Rev. Lett.* **87** 173601
- [2] Moiseev S A, Tarasov V F and Ham B S 2003 Quantum memory photon echo-like techniques in solids *J. Opt. B: Quantum semiclass. Opt.* **5** S497
- [3] Kurnit N A, Abella I D and Hartmann S R 1964 Observation of a photon echo *Phys. Rev. Lett.* **13** 567
- [4] Wootters W K and Zurek W H 1982 A single quantum cannot be cloned *Nature* **299** 802
- [5] Togan E, *et al.*, 2010 Quantum entanglement between an optical photon and a solid-state spin qubit *Nature* **466** 730
- [6] Macfarlane M R and Shelby R M 1987 Coherent transient and holeburning spectroscopy of rare earth ions in solids, in Spectroscopy of solids containing rare earth ions Kaplyanski, A. and Macfarlane, R. M., eds. (North-Holland)
- [7] Riedmatten H de *et al.*, 2008 A solid-state light-matter interface at the single-photon level. *Nature* **456**, 773

- [8] Tittel W *et al.*, 2010 Photon-echo quantum memory in solid state systems *Laser and Photon. Rev.* **4** 244
- [9] Hétet G *et al.*, 2008 Electro-Optic Quantum Memory for Light Using Two-Level Atoms *Phys. Rev. Lett* **100** 023601
- [10] Hedges M P, Longdell J J, Li Y and Sellars M J 2010 Efficient quantum memory for light *Nature* **465**, 1052
- [11] Ham B S 2011 Atom phase controlled noise-free photon echoes *arXiv:1101.5480v2*
- [12] Ham B S 2016 Collective atom phase controls in photon echoes for quantum memory applications I: Population inversion removal *arXiv:1612.00115*
- [13] Duan L –M, Lukin M D, Cirac J I and Zoller P 2001 Long-distance quantum communication with atomic ensembles and linear optics *Nature* **414** 413
- [14] Sangouard N, Simon C, Riedmatten de H and Gisin N 2011 Quantum repeaters based on atomic ensembles and linear optics *Rev. Mod. Phys.* **83** 33
- [15] Longdell J J, Fraval E, Sellars M J and Manson N B 2005 Stopped light with storage times greater than one second using electromagnetically induced transparency in a solid *Phys. Rev. Lett* **95** 063601
- [16] Ham B S 2009 Ultralong quantum optical data storage using an optical locking technique *Nature Photon.* **3** 518
- [17] Ham B S 2012 Coherent control of collective atom phase for ultralong, inversion-free photon echoes. *Phys. Rev. A* **85**, 031402(R)
- [18] Langer L *et al.*, 2014 Access to long-term optical memories using photon echoes retrieved from semiconductor spin *Nature Photon.* **8** 851
- [19] Ham B S 2012 Atom phase-locked coherence conversion using optical locking for ultralong photon storage beyond the spin T2 constraint *New J. Phys.* **14** 013003
- [20] Damon V *et al.*, 2011 Revival of silenced echo and quantum memory for light *New. J. Phys.* **13** 093031
- [21] Arcangeli A, Ferrier A and Goldner Ph. 2016 Stark echo modulation for quantum memories *Phys. Rev. A* **93**, 062303
- [22] McAuslan D L *et al.*, 2011 Photon-echo quantum memories in inhomogeneously broadened two-level atoms *Phys. Rev. A* **84**, 022309
- [23] Ham B S 2017 Gaussian beam profile effectiveness on double rephasing photon echoes *arXiv:1701.04291*
- [24] Ham B S 2010 Control of photon storage time using phase locking *Opt. Exp.* **18** 1704
- [25] Hahn J and Ham B S 2011 Rephasing halted photon echoes using controlled optical deshelving *New J. Phys.* **13** 093011
- [26] Afzelius M *et al.* 2010 Demonstration of atomic frequency comb memory for light with spin-wave storage *Phys. Rev. Lett.* **104** 040503
- [27] Zhong M *et al.* 2015 Optical addressable nuclear spin in a solid with a six-hours coherence time *Nature* **517** 177
- [28] Sargent III, M., Scully, M. O. & Lamb Jr., W. E. *Laser Physics* (Addison-Wesley, 1974).
- [29] Hahn E L and Shiren N S 1971 Application of the area theorem to phonon echoes *Phys. Lett. A* **37** 265
- [30] Fraval E, Sellars M J and Longdell J J 2004 Method of Extending Hyperfine Coherence Times in $\text{Pr}^{3+}:\text{Y}_2\text{SiO}_5$ *Phys. Rev. Lett.* **92** 077601